Expert Opinion

Thermally targeted delivery of chemotherapeutics and anti-cancer peptides by elastin-like polypeptide

Drazen Raucher†, Iqbal Massodi & Gene L Bidwell III
†*University of Mississippi Medical Center, Department of Biochemistry, 2500 North State Street, Jackson, MS 39216, USA*

Current chemotherapy treatment of solid tumors is limited due to a lack of specific delivery of the drugs to the tumor, leading to systemic toxicity. Therefore, it is necessary to develop targeted cancer therapies and tumor-targeted drug carriers. The authors review the development of elastin-like polypeptide (ELP) as a potential carrier for thermally targeted delivery of therapeutics. The authors searched Medline for articles concerning the application of ELP as a drug delivery vector for small molecule drugs and therapeutic peptides. ELP has been demonstrated to be a promising thermally targeted carrier. Further examination of the *in vivo* biodistribution and efficacy will provide the necessary data to advance ELP technology toward the ultimate goal of human therapeutics.

Keywords: c-Myc, doxorubicin, elastin-like polypeptide, p21, therapeutic peptides, thermal targeting

Expert Opin. Drug Deliv. (2008) 5(3):353-369

1. Introduction

Major limitations of current cancer therapy are poor drug efficacy and extensive toxicity to non-cancerous tissues. Classical chemotherapy drugs work by killing actively dividing cells nonspecifically, which makes them highly toxic when used in the doses needed to eliminate cancer cells. This problem may be overcome by a twofold approach: i) the development of drug carriers capable of delivering the drug specifically to the tumor site; and ii) the development of new, targeted therapeutic agents which are specifically toxic to cancer cells, while sparing normal tissues. The first approach may be achieved using thermally responsive drug carriers, capable of specifically delivering or releasing the drug at the tumor site where local hyperthermia is applied. The second approach uses targeted drugs that work by attacking the cellular oncogenes which have become mutated or overexpressed during the cancer cells' oncogenic transformation. Recent solutions of the three-dimensional structure of many oncogenic proteins, rational design based on known protein–protein interactions and the use of large library screens has yielded the discovery of many bioactive peptides which can be used to target the oncogenic proteins' cellular activities [1-9]. These peptides bind and inhibit specific oncogenes [1,10] or induce apoptosis [8,9]. Although they can be very specific for the cancer cells, peptide therapy is severely limited by poor pharmacokinetic parameters *in vivo* [11,12]. This may be overcome by attaching the peptides to a macromolecular carrier [13]. This review describes the use of a thermally responsive polypeptide carrier for hyperthermia targeted delivery of small molecule chemotherapeutics and tumor-specific therapeutic peptides. This thermally responsive drug carrier can be administered systemically, and, due to its physical property of hyperthermia-induced aggregation, it will accumulate *in vivo*

informa
healthcare

at sites where mild, focused heat is applied. Its use as a vector for therapeutic peptides is especially attractive because, in addition to physical targeting to the tumor site by application of external hyperthermia, the peptides are molecularly targeted to the tumor due to their oncogene inhibition. The result is a macromolecular peptide delivery vector with two layers of target specificity.

Elastin-like polypeptide (ELP) is a protein-based biopolymer made of a repeating sequence of the amino acids VPGXG, where X is any amino acid except proline [14]. ELP is an ideal delivery vector for chemotherapeutic drugs and therapeutic peptides for several reasons. First, ELP is genetically encoded [15]. This gives the designer unlimited control of the sequence and molecular weight to an extent that is impossible with chemically synthesized polymers. The molecular weight and polydispersity are important because they control the residence time of polymers in circulation and their deposition in tumor beds [16,17]. The genetically encoded nature of ELP makes the addition of reactive sites for drug conjugation easy, and the number and location of these sites can be tightly controlled. Also, being genetically encoded makes ELP especially useful for the delivery of therapeutic peptides. While classical approaches use complex chemical modifications to attach drugs to carriers, ELP may be attached to therapeutic peptides using simple molecular biology techniques [18]. Second, ELP can be expressed in *E. coli*. This gives the user access to large quantities of the pure therapeutic. After expression and lysis of the bacteria, ELP is separated from other soluble *E. coli* proteins by inducing aggregation of ELP by raising the solution temperature, then collecting the aggregated protein by centrifugation. Repeated centrifugation steps above and below the aggregation temperature yield ELP at very high purity and excellent yield [18,19]. Third, ELP is a macromolecule. Macromolecular drug carriers passively accumulate in tumor tissue due to its high vascular permeability and poor lymphatic drainage, a phenomenon known as the enhanced permeability and retention effect [20-23]. Also, macromolecular carriers are known to increase drug half-lifes in circulation [24,25], reduce non-specific toxicity [26-28], and overcome multidrug resistance [29-32]. Fourth and most important, ELP is thermally responsive. Below a critical solution temperature called the transition temperature (T_t), ELP polymers are solvated monomers. When a solution of ELP molecules is raised above the T_t, the polypeptide undergoes a hydrophilic to hydrophobic phase transition, becomes desolvated and forms large polypeptide aggregates [14,33]. The T_t of ELP is dependent on the polypeptide's molecular weight and on the hydrophobicity of the amino acids in the X position, making the T_t tunable to any desired temperature by altering the mole fraction of the amino acids X [14]. Furthermore, the ELP phase transition is fully reversible upon lowering of the temperature below the T_t. This phase transition can be exploited for thermally targeted drug delivery. ELPs can be designed with a T_t slightly above normal body temperature. When injected intravenously, ELPs circulate systemically and eventually are cleared from circulation. However, at the tumor site where local hyperthermia is applied, ELPs aggregate and accumulate [15,34,35].

Doxorubicin (Dox) is an anthracycline antibiotic that was first isolated from the fungus *Streptomyces peucetius* by the Farmitalia Research Laboratories of Milan in the early 1960s, and first approved for clinical use in the US in 1974. Dox has broad applicability as an antitumor agent for the treatment of many types of solid tumors and hematologic malignancies. Dox cytotoxicity occurs through several different mechanisms. The drug intercalates into DNA and blocks DNA replication and transcription [36]. Additionally, Dox binds to topoisomerase II (topo II) and stabilizes the topo II cleavage complex, leading to double-strand breaks [37] and apoptosis [38]. Dox also produces free radicals [39] which can induce oxidative damage to cell membranes by lipid peroxidation [40,41], and Dox can even be cytotoxic without entering the cell [42]. Although it has broad clinical applications, the use of Dox is severely limited by its strong adverse side effects, the most prominent and dose limiting of which is cardiotoxicity [43-47]. Therapy with Dox is also severely limited by the development of drug resistance by the tumor cells [48]. The toxicity and susceptibility to cellular resistance mechanisms may be overcome by attaching Dox to a macromolecular drug carrier. This review will describe the attachment of Dox to ELP for thermally targeted delivery and evasion of multidrug resistance.

In the past few years, the field of therapeutic peptides has made major advances. Many peptides which specifically inhibit the proliferation of cancer cells have been discovered through rational design based on three-dimensional structures [1,49] or known protein–protein interaction domains [3,4,50-52], through screening of random peptide libraries [53], or through modification of naturally occurring peptides with antibiotic properties [5-7,54]. These inhibitory peptides work through diverse mechanisms. One class of recently discovered peptides inhibits oncogene activity by blocking a critical interaction between a protein and its dimerization partner. These include the inhibition of dimeric transcription factors [1,2] and the interruption of signal transduction cascades by blocking interactions needed for phosphorylation events [3,4]. Other varieties of inhibitory peptides work by mimicking natural inhibitors of cell proliferation [5-7]. These include peptides which mimic cyclin-dependent kinase (Cdk) inhibitory proteins, which block progression through the cell cycle [50]. Finally, inhibitory peptides may directly induce cell death by induction of apoptosis. Peptides of this type have been described which induce cytochrome C release from the mitochondrial membrane [6]; cause ionic imbalance by making pores in the plasma membrane [55,56]; activate the pro-apoptotic members of the Bcl-2 protein family, including Bax, Bim and BID [8,9]; and replace the function of the p53 protein which is lost in

many cancer cell lines due to mutation or deletion [52]. Because of the diversity of the available therapeutic peptides and their specificity for cellular targets, this field offers great potential for new and improved therapeutics. However, peptide therapies are severely limited due to rapid degradation and/or clearance and poor tumor uptake *in vivo*. To overcome these hurdles, therapeutic peptides can be attached to a polymer carrier to increase the plasma half-life and tumor deposition. This review will focus on the use of ELP to deliver two therapeutic peptides, one that inhibits the function of the oncogenic transcription factor c-Myc [18] and one that mimics the Cdk inhibitor p21 [57].

2. Body

2.1 The potential of elastin-like polypeptide for drug delivery *in vivo*

When applied *in vivo*, systemically injected ELP remains soluble and freely circulates at normal body temperature. However, at localized sites where hyperthermia is applied to raise the tissue above the ELP's T_t, the polypeptide aggregates and accumulates. In a study by Meyer *et al.* [15], mice bearing SKOV-3 ovarian tumors implanted under a window chamber in the back accumulated 54% more thermally responsive ELP after heating for 50 min as compared to a non-thermally responsive control, as assessed by fluorescence videomicroscopy. Additionally, mice bearing D-45MG glioma tumors implanted subcutaneously in the flank accumulated 34% more thermally responsive ELP after heating, as assessed by radioactive counting. The authors further concluded that 60% of the total increase in ELP uptake with hyperthermia was attributed to ELP aggregation, and 40% of the total increase was due to the physiological effects of hyperthermia [15]. More recently, a study by Liu *et al.* [58] showed that ELP was cleared from mouse circulation in a biexponential manner after intravenous injection, with half-lifes of 7.32 min and 8.37 h for the two phases. Accumulation of a thermally responsive ELP in FaDu xenografts grown in the flank of these mice increased 1.8-fold compared to unheated tumors and 1.5-fold compared to a thermally non-responsive ELP [34]. Additionally, it was reported that repeated heating and cooling cycles can further increase ELP accumulation in tumor tissue [35]. Attachment of drugs or therapeutic peptides to ELP offers the capability to specifically deliver these therapeutics to the desired tissue by focused application of externally applied hyperthermia. The use of hyperthermia has an added advantage of increasing vessel permeability [59-61]. The ELP-based drug delivery system described here combines the advantages of macromolecular delivery, hyperthermia and thermal targeting.

2.2 Design of the ELP-based drug delivery vectors

The ELP-based drug delivery vectors were designed to include two versions of ELP. ELP1 is a 59.4 kDa polypeptide with 150 repeats of the VPGXG sequence and the X position is occupied by Val, Gly and Ala in a 5:3:2 ratio. ELP1 was designed to have a transition temperature just above normal body temperature (**Figure 1B**) for use as a thermally targeted drug carrier. A second set of polypeptides contains the ELP2 sequence, which is 160 repeats of VPGXG, where X is Val, Gly and Ala in a 1:7:8 ratio [15]. The molecular weight of ELP2 is similar to that of ELP1, but ELP2 does not undergo its phase transition at the hyperthermia temperatures used for thermal targeting ($T_t \approx 65°C$). This makes ELP2 a useful control for discerning the effects of the ELP phase transition from non-specific effects of hyperthermia [15,62,63].

Large macromolecules such as ELP are inherently impermeable to the plasma membrane. In order to increase the intracellular uptake of the ELP-based peptide delivery vectors, a cell penetrating peptide is included at the N-terminus of each construct. These short peptides (7 – 25 amino acids), are known to enhance the uptake of large molecules into the cell interior. Finally, ELP is modified at its C-terminus with the drug or inhibitory peptide of choice (**Figure 1A**).

2.3 Use of cell penetrating peptides to enhance the intracellular delivery of ELP

A macromolecular carrier has to overcome various transport barriers in order to exhibit therapeutic efficacy. The plasma membrane, which is impermeable to large, hydrophilic compounds, makes the intracellular delivery of these macromolecular polypeptides inefficient. One approach to overcome this problem is to couple the macromolecule to a cell penetrating peptide (CPP). A number of CPPs of varying chemical composition have been characterized for their ability to translocate different cargoes across cell membranes [22,64].

ELPs are genetically encoded, and synthesis of ELPs by recombinant DNA methods provides precise control over the ELP sequence. To generate fusion polypeptides containing ELP, the original coding sequence for ELP was modified by attaching different CPPs at the N-terminus of ELP. In order to optimize ELP intracellular delivery, Massodi *et al.* [57] tested three of the most widely used CPPs: the penetratin peptide (Pen), which is derived from the Drosophila transcription factor Antennapedia (Antp) [65], the Tat peptide derived from the HIV-1 Tat protein [66], and a hydrophobic peptide (MTS) derived from the Kaposi fibroblast growth factor signal peptide [67]. In order to evaluate the efficiency of membrane transduction, the authors labeled each CPP–ELP construct with fluorescein at an engineered, C-terminal cysteine residue. Various concentrations of the fluorescently labeled CPP–ELPs were incubated with HeLa cells at 37°C for 1 h, and the amount of polypeptide associated with the cells was determined by flow cytometry. All CPPs tested significantly enhanced the cellular uptake of ELP. At the highest concentration tested,

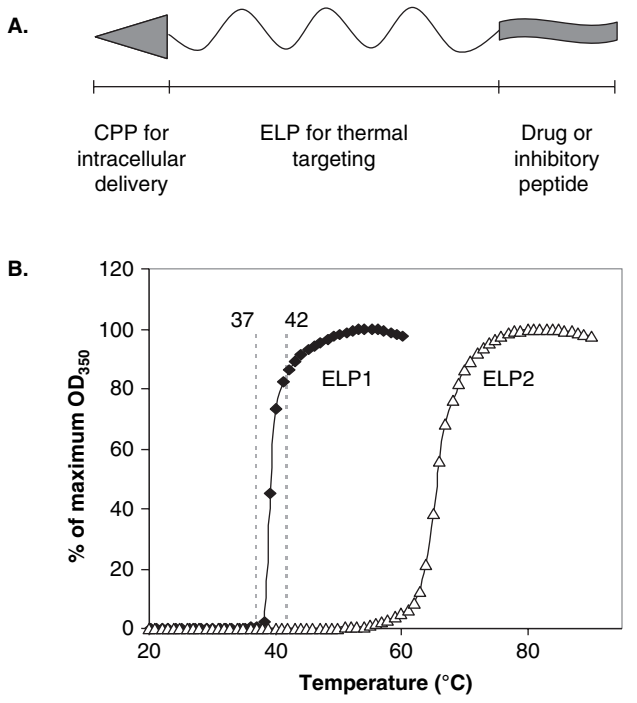

Figure 1. Design and thermal properties of ELP-based drug carriers. A. The ELP-based drug carriers are made of three functional domains. A cell penetrating peptide (CPP) at the N-terminus enhances uptake of the macromolecule across the plasma membrane. The ELP domain is a thermally responsive pentapeptide repeat. At the C-terminus, a therapeutic molecule is attached, either via a chemical linker for small molecule drugs or via gene fusion for peptide therapeutics. **B.** Thermal aggregation of ELP due to its inverse phase transition. Below a characteristic transition temperature (T_t), ELP is soluble. When the solution is raised above the T_t, ELP becomes desolvated and aggregates. The T_t is measured by monitoring the turbidity of a solution while heating at 1°C/minute. ELP1 undergoes its phase transition at 40°C, making it ideal for thermal targeting with mild hyperthermia (42°C). ELP2 has a much higher T_t (65°C), making it a useful control for distinguishing the effects of ELP aggregation from non-specific effects of hyperthermia.
ELP: Elastin-like polypeptide.

the enhanced cellular uptake by Tat and MTS was about twofold. However, the Pen peptide enhanced the cellular uptake of ELP about 15-fold [57]. Using a trypan blue quenching assay, it was confirmed that the enhanced cellular uptake observed was due to internalization of the CPP–ELP polypeptides. Only 25 – 35% of the polypeptides were internalized in the first hour, but this percentage increased to 40 – 50% towards the 2 h and 4 h period. 24 h after treatment, nearly 60 – 80% of all polypeptides were internalized. These results were confirmed using confocal fluorescence microscopy to demonstrate a cytoplasmic distribution for all CPP–ELPs tested.

In order to elucidate the mechanism of CPP–ELP uptake, endosomal participation was analyzed. It has been reported that various CPPs enter the cells via endocytosis. Previous studies have shown that low temperature and cellular energy depletion reduced cellular uptake of CPP–avidin complexes [68]. Another study showed that incubation at 4ºC strongly inhibited uptake of Tat fusion proteins, suggesting that, unlike short cationic peptides, full length protein internalization requires energy [69]. Since low temperature and energy depletion severely affects endocytotic uptake, their role was determined in the uptake of CPP–ELPs in HeLa cells. Incubation with cells at 4°C, or ATP depletion with 2-deoxy-D-glucose, significantly reduced the uptake of all CPP–ELPs tested [57].

To further explore the role of endocytosis in the uptake of CPPs, the effect of endocytotic inhibitors was examined. Endocytosis occurs via many different mechanisms, such as clathrin-dependent and clathrin-independent [70-72]. Clathrin-dependent endocytosis involves formation of membrane invaginations which are coated with clathrin and are also known as clathrin-coated pits. It has been reported that formation of clathrin-coated pits can be inhibited by a hyperosmolar sucrose solution [73]. Incubation of HeLa cells with 0.45 M sucrose inhibited the uptake and internalization of ELP and Tat-ELP slightly, while exerting a nearly 50% reduction in internalization of MTS–ELP and Pen-ELP [57]. These results indicate that clathrin-mediated endocytosis plays a part in the internalization of the CPP–ELPs. Another mechanism in the endocytotic pathway is the clathrin-independent caveolae dependent pathway. Caveolae are small (50 – 100 nanometer) invaginations of the plasma membrane which are rich in proteins as well as lipids such as cholesterol and sphingolipids and play a role in endocytosis [74]. Methyl-β-cyclodextrin (MβCD) treatment in cells leads to the extraction of the membrane cholesterol and flattening of the plasma membrane. Preincubation of cells with 5 mM MβCD for 30 min at 37ºC did not show any significant change in the internalization of CPP–ELPs [57]. This experiment suggests that internalization of CPP–ELPs occurs via a caveolae-independent pathway.

2.4 Delivery of doxorubicin by ELP

Use of the chemotherapeutic Dox is limited by severe side effects, including cardiotoxicity, and by the development of drug resistance by cancer cells. Dox has been fused to ELP in an attempt to overcome these limitations by achieving thermally targeted delivery of Dox to the tumor site. Dreher *et al.* [75] examined an ELP–Dox fusion for its ability to kill cancer cells *in vitro*. Dox was covalently attached to ELP through an acid labile hydrazone linker. Attachment of Dox to ELP lowered the T_t by about 10°C, which made thermal targeting with the ELP–Dox conjugate impossible. However, the authors did show that the ELP–Dox conjugate was cytotoxic to FaDu squamous carcinoma cells, and the potency of the ELP–Dox was similar to that of free Dox. Interestingly, the authors observe that the ELP–Dox was internalized by the FaDu cells, but it localized almost exclusively to the cytoplasm.

This is in contrast to free Dox, which localized almost exclusively to the nucleus, and the authors suggest that ELP–Dox and free Dox kill cells via different mechanisms. This is consistent with other studies of polymer-delivered Dox [76,77]. This study was extended by Furgeson *et al.* [78] who modified the attachment of Dox to ELP by using different pH-sensitive hydrazone linkers. The authors were able to optimize the release of Dox from ELP at low pH using this method, but these constructs have not been tested for relative cytotoxicity to date.

An alternative ELP-based Dox delivery molecule was described by Bidwell *et al.* [79] in which Dox was attached to ELP via a cleavable peptide linker, and the Tat CPP was added to the construct to enhance its cellular uptake (Tat–ELP–GFLG–Dox). This construct also varied from previously published versions in that it had a transition temperature of 40°C, ideal for thermal targeting. WP936 is a thiol reactive Dox derivative obtained by conjugating a maleimido moiety via a linker with the amino group at the C-3′ position. WP936 was covalently attached to the sulfur of an engineered, C-terminal cysteine residue by nucleophilic addition. The terminal cysteine was connected to ELP via a GFLG tetrapeptide linker to allow intracellular drug release by lysosomal proteases (**Figure 2A**) [80].

The cellular uptake of Tat–ELP–GFLG–Dox was assessed in MES-SA uterine carcinoma cells by measuring the Dox fluorescence by flow cytometry after cell treatment. It was shown that cellular uptake was increased about threefold by inclusion of the Tat peptide, and the cellular uptake of Tat–ELP1–GFLG–Dox was increased twofold further by causing the polypeptide to aggregate with hyperthermia treatment (**Figure 2B**). Uptake of a control polypeptide containing the non-thermally responsive ELP2 moiety was not increased by hyperthermia treatment, indicating that the increase seen with the ELP1-containing construct was due to aggregation of ELP. Internalization and subcellular localization of Tat–ELP–GFLG–Dox was confirmed using confocal microscopy to visualize the Dox fluorescence. Immediately following a 1 h exposure to Tat-ELP1-GFLG-Dox at 37°C, cytoplasmic staining with a punctate perinuclear accumulation was evident (**Figure 2C**, top left). 24 h after the treatment was removed, the polypeptide was distributed diffusely throughout the cytoplasm (**Figure 2C**, top right). When Tat-ELP1-GFLG-Dox treatment was combined with hyperthermia, large membrane blebs indicative of apoptosis were visible 1 h after treatment (**Figure 2C**, bottom left) and cell morphology was completely disrupted 24 h after the hyperthermia treatment (**Figure 2C**, bottom right). Little, if any, Dox was present in the nucleus after Tat–ELP–GFLG–Dox treatment. This observation is consistent with that of Dreher *et al.* [75], who proposed that ELP-delivered Dox may be functioning by a different mechanism from the free drug. Tat-ELP1-GFLG-Dox was able to inhibit proliferation of the MES-SA cells, as indicated by a cell counting assay 72 h after a 1 h exposure to the polypeptides. **Figure 2D** shows that Tat-ELP1-GFLG-Dox was able to inhibit the proliferation of MES-SA cells at 37°C with an IC_{50} (50% inhibitory concentration) of 20 μM (top panel). When treatment was combined with hyperthermia (42°C), the potency of Tat-ELP1-GFLG-Dox was increased 20-fold (IC_{50} = 1 μm). The non-thermally responsive control Tat-ELP2-GFLG-Dox inhibited proliferation equally at both treatment temperatures, and its potency was not significantly different from Tat–ELP1–GFLG–Dox at 37°C (**Figure 2D**, bottom panel).

Another inherent limitation on the use of small molecule chemotherapeutics such as Dox is the ability of cancer cells to develop resistance to these drugs. One of the most prominent resistance mechanisms involves drug efflux from the cells by expression of P-glycoprotein (P-gp). To overcome this mechanism of resistance, small molecule drugs are often attached to polymeric carriers, which makes them poor substrates for P-gp efflux. Bidwell *et al.* demonstrated that the ELP-bound Dox polymer Tat–ELP–GFLG–Dox was able to bypass P-gp mediated drug efflux and accumulate in cells expressing high levels of P-gp [81]. As shown in **Figure 3A**, free Dox is much less potent (70-fold) in the P-gp positive cell line MES-SA/Dx5 as compared to the P-gp negative MES-SA cell line (top left). However, the ELP-bound form of the drug (Tat–ELP–GFLG–Dox) was equally potent in both cell lines (top right). This result was confirmed in another P-gp expressing cell line, NCI/ADR-RES (bottom panel). In order to confirm that Tat–ELP–GFLG–Dox was evading P-gp mediated drug efflux, the cellular Dox level was determined relative to the P-gp level in MES-SA/Dx5 cells by immunofluorescence microscopy and flow cytometry. **Figure 3B** shows that when treated with Dox, two populations of MES-SA/Dx5 cells emerged due to the fact that, at least immediately after treatment, Dox can inhibit transcription of the P-gp mRNA [32]. Those cells with high P-gp expression accumulate very little Dox, while those with lower P-gp expression accumulate much more Dox (top right). Tat–ELP–GFLG–Dox, however, accumulates equally in all cells (bottom panel). This result was confirmed by immunofluorescence microscopy (**Figure 3C**). Cells with high levels of P-gp do not contain detectable levels of Dox (top panel, black arrows) and cells with little P-gp expression do contain Dox (top panel, white arrows). In contrast to the free drug, Tat–ELP–GFLG–Dox accumulates equally in all cells, including those with high expression levels of P-gp (bottom panel, black arrows). The ability of Tat–ELP–GFLG–Dox to bypass P-gp mediated efflux was further confirmed by quantifying the cellular Dox level in P-gp positive and P-gp negative cells by HPLC following treatment with free Dox or Tat–ELP–GFLG–Dox. **Figure 3D** shows that immediately after drug exposure, free Dox was present in MES-SA/Dx5 cells at only about half the level found in MES-SA cells. And, 24 h later, free Dox was almost undetectable in MES-SA/Dx5 cells. Tat–ELP–GFLG–Dox, on the other hand,

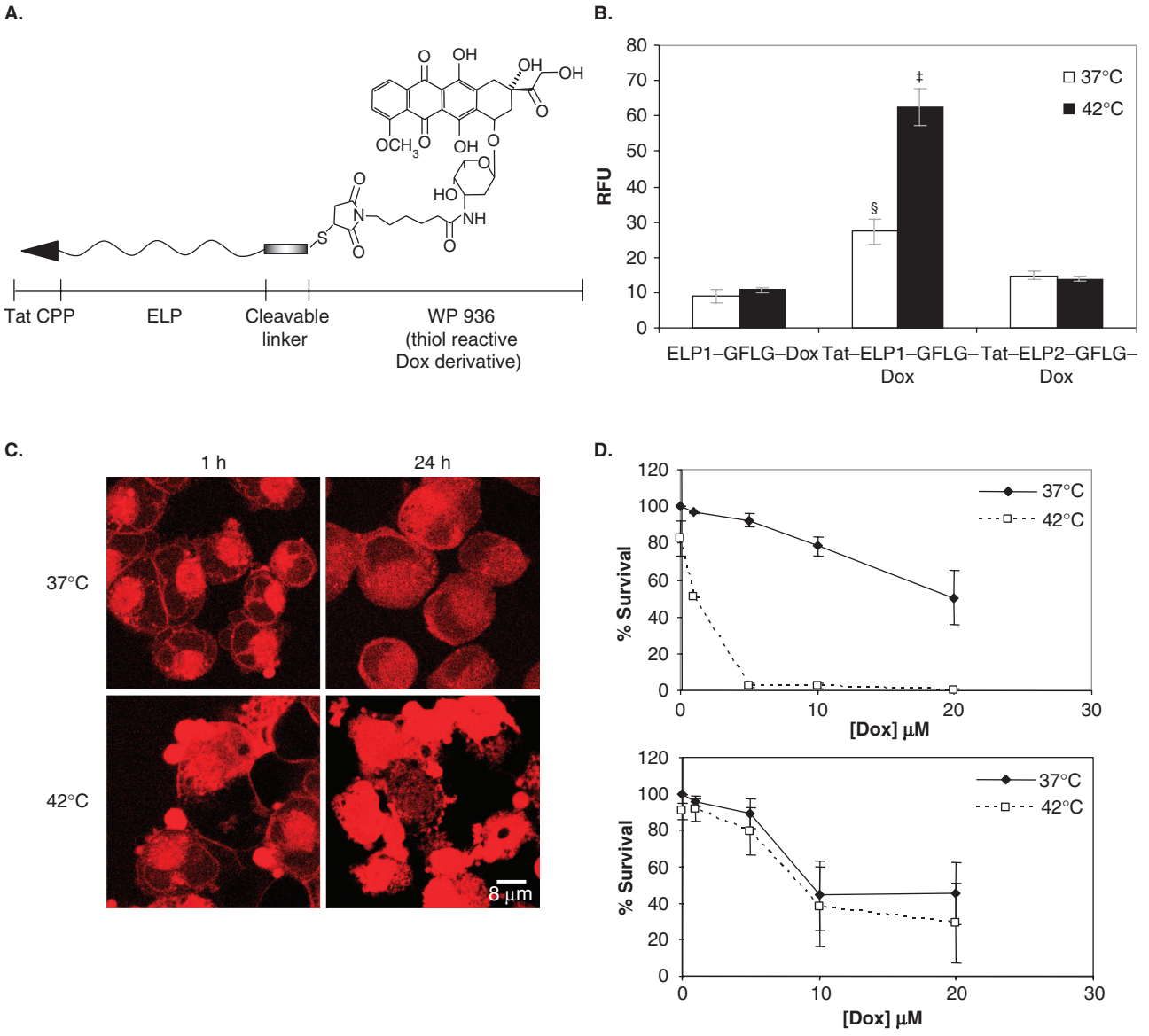

Figure 2. Thermally targeted delivery of doxorubicin by fusion with ELP. A. Schematic of the ELP-based Dox delivery vector. The polypeptide contains the Tat cell penetrating peptide at the N-terminus, the thermally responsive ELP, the GFLG cathepsin cleavage sequence and a C-terminal cysteine for conjugation of the thiol reactive Dox derivative WP936. **B.** Cellular uptake of Dox labeled ELP. MES-SA uterine sarcoma cells were incubated with Dox labeled constructs (20 µM in cell culture media) for 1 h at 37°C or 42°C. The Dox fluorescence intensity was determined using flow cytometry and is expressed in relative fluorescence units (RFU). The data represents the mean of at least three experiments (error bars, SEM). §Significant difference compared with ELP1–GFLG–Dox at 37°C. ‡Significant difference compared with Tat–ELP1–GFLG–Dox at 37°C ($p < 0.0001$, one-way ANOVA, $p < 0.05$, Scheffe's test). **C.** Intracellular localization of Tat–ELP–GFLG–Dox. Confocal fluorescence images of MES-SA cells were collected 1 h and 24 h after a 1 h exposure to Tat–ELP1–GFLG–Dox (10 µM in cell culture media) at 37°C or 42°C. PMT voltages were decreased for collection of 42°C images. Therefore, the image intensity does not reflect the actual level of Dox in the cells. **D.** Inhibition of cell proliferation by Tat–ELP–GFLG–Dox. MES-SA cells were exposed to varying concentrations of Tat–ELP1–GFLG–Dox (top panel) or Tat–ELP2–GFLG–Dox (bottom panel) for 1 h at 37°C or 42°C, and the cells were counted after 72 h. The data represent an average of at least three experiments (bars, SEM).
ELP: Elastin-like polypeptide; SEM: Standard error of the mean.

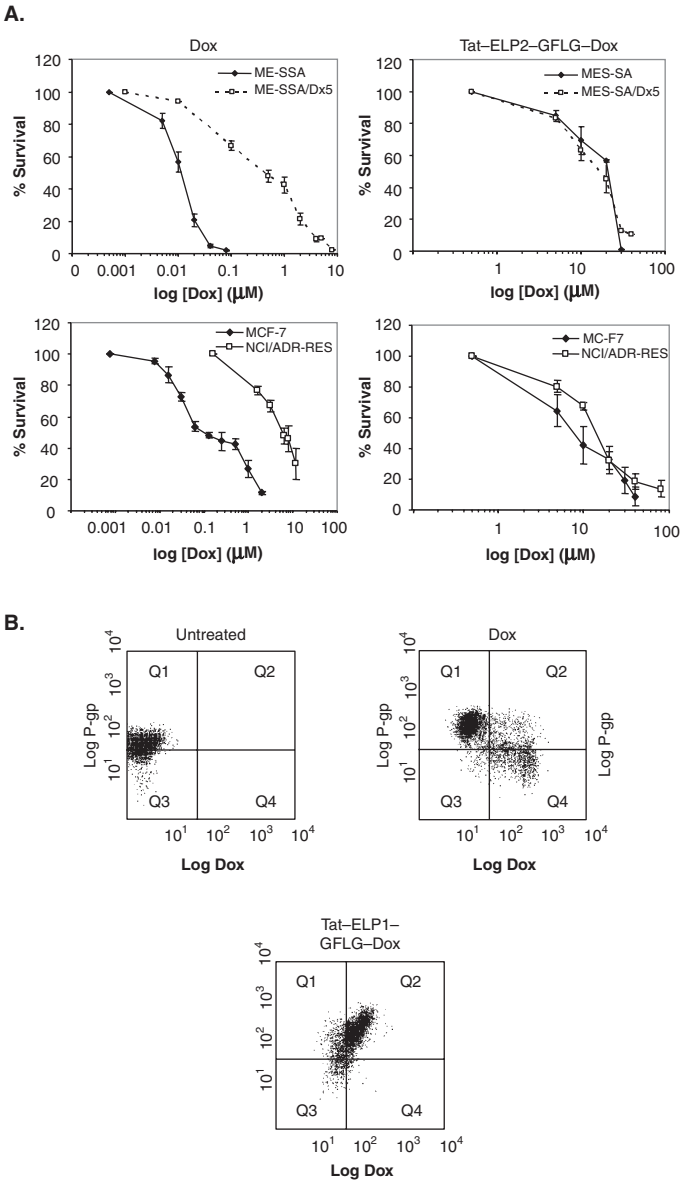

Figure 3. Delivery of Dox in multidrug resistant cells using Tat–ELP–GFLG (continued). A. Cytotoxicity in sensitive and resistant cell lines. The cytotoxicity of Dox (left panel) and Tat-ELP2-GFLG-Dox (right panel) was determined by exposing MES-SA and MES-SA/Dx5 cells (top panel) to the drugs at the indicated concentrations for 72 h. The assay was repeated in sensitive MCF-7 and multidrug resistant NCI/ADR-RES cell lines (bottom panel). The data represent the average of at least three experiments. Bars, SEM. **B.** Correlation of Dox staining and P-gp expression by fl ow cytometry. MES-SA/Dx5 cells were treated for 24 h with drug-free control media (top, left), 10 μM Dox (top, right) or 10 μM Tat-ELP1-GFLG-Dox (bottom). The intrinsic Dox fl uorescence was detected in channel FL3, and P-gp was stained with a PE-Cy7 labeled antibody and detected in channel FL5. The data are a representative sample of at least three experiments.

ELP: Elastin-like polypeptide; SEM: Standard error of the mean.

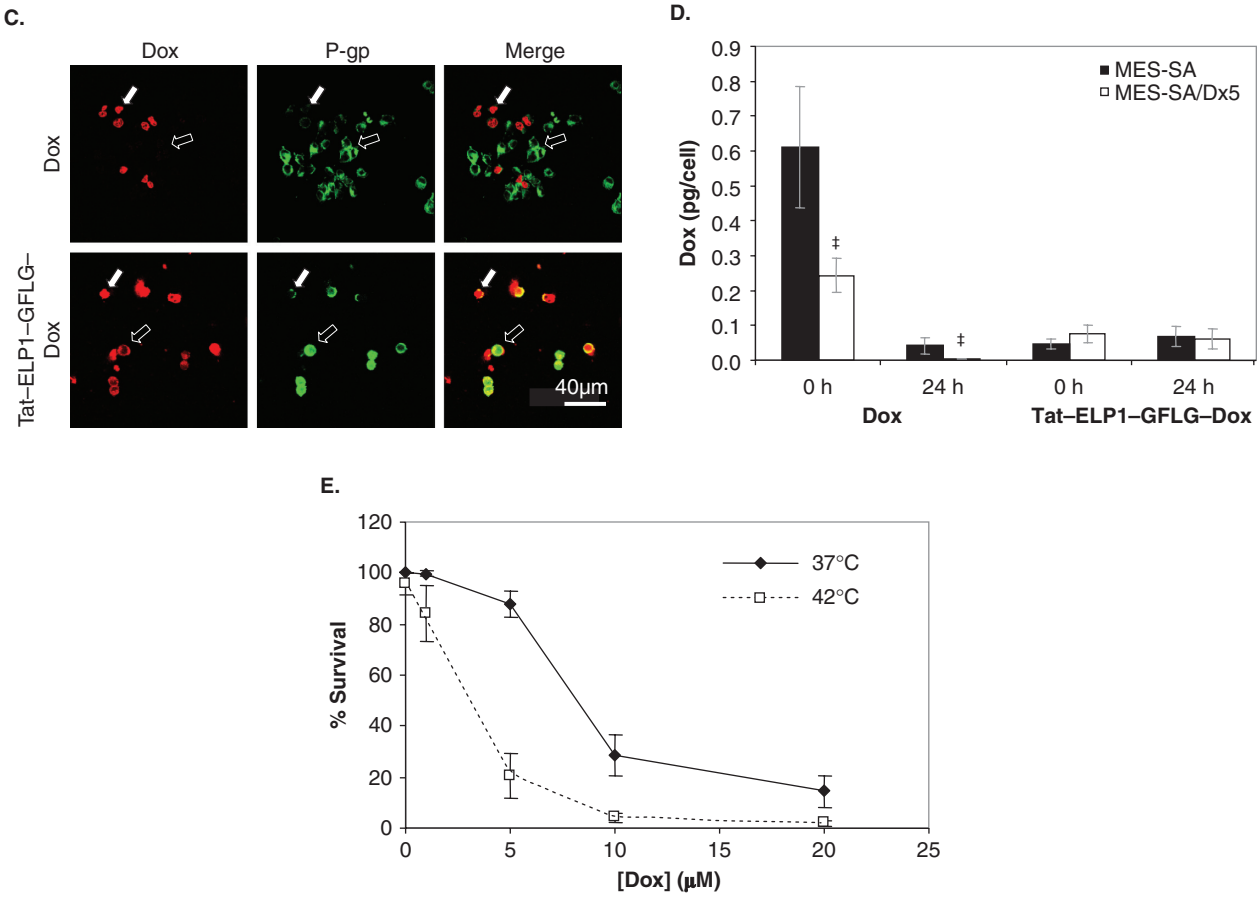

Figure 3. Delivery of Dox in multidrug resistant cells using Tat–ELP–GFLG (continued). C. Correlation of Dox staining and P-gp expression by immunofluorescence microscopy. Following 24 h treatment with Dox (top panel) or Tat–ELP1–GFLG–Dox (bottom panel), MES-SA/Dx5 cells were fixed and immunostained for P-gp expression. The intrinsic Dox fluorescence is shown in red (left panel), and the Alexa 633 stained P-gp fluorescence is shown in green (middle panel). The images were overlaid to determine if P-gp expression and Dox staining co-exist (right panel). **D.** HPLC assay for Dox levels. The level of Dox or Tat–ELP–GFLG–Dox was determined in MES-SA and MES-SA/Dx5 cells by HPLC. Cells were lysed 0 h or 24 h after a 5 h exposure to Dox or Tat–ELP1–GFLG–Dox, the drug was extracted, and levels of Dox and the internal extraction standard daunorubicin (Dnr) were determined by HPLC. The average drug level per cell was determined by fitting the area under each peak to a standard curve of Dox, hydrolyzed Tat–ELP1–GFLG–Dox, or Dnr and averaging at least three experiments. Bars, SD. ‡Differences between MES-SA and MES-SA/Dx5 were statistically significant as assessed by a Student's *t*-tests with a level of significance of $p < 0.05$. **E.** Enhancement of Tat–ELP1–GFLG–Dox potency using hyperthermia in Dox resistant cells. MES-SA/Dx5 cells were exposed to the indicated concentration of Tat–ELP1–GFLG–Dox for 1 h at 37 or 42°C, then the polypeptide was washed away and the cells were allowed to proliferate for 72 h. Cell number was determined by Coulter counting.
ELP: Elastin-like polypeptide; SD: Standard deviation.

was present in equal amounts in both MES-SA and MES-SA/Dx5 cells immediately after treatment, and the cellular Tat–ELP–GFLG–Dox levels were stable for 24 h. It is interesting to note that the level of Tat–ELP–GFLG–Dox initially present in both cell lines is far less than the level of Dox. This is indicative of the disparate mechanisms by which the drugs gain cellular entry. Free Dox is sufficiently small and hydrophobic to enter the cells by passive diffusion, while Tat–ELP–GFLG–Dox enters the cells by endocytosis [57]. This reduced initial drug level likely explains why Tat–ELP–GFLG–Dox is less potent than free Dox in both cell lines (**Figure 2A**). Although it leads to lowered cellular drug levels and lower potency, the endocytic mechanism of entry allows Tat–ELP–GFLG–Dox to evade the P-gp efflux pump.

It was also shown that the potency of Tat–ELP–GFLG–Dox could be increased using hyperthermia treatment. The IC_{50} of Tat-ELP1-GFLG-Dox was reduced 2.8-fold by combining a 1 h cell exposure to the polypeptide with hyperthermia (**Figure 3E**). Such an enhancement was not seen with the control Tat-ELP2-GFLG-Dox polypeptide (data not shown), indicating that the enhancement was due to ELP aggregation. These initial *in vitro* data suggest that this treatment mechanism may prove useful in drug resistant tumors *in vivo*.

2.5 Delivery of a c-Myc inhibitory peptide by ELP

c-Myc is a transcriptional regulator which controls cell growth, proliferation, apoptosis and tumorigenesis. It has been shown that deregulated expression of c-Myc is associated with numerous types of human cancers, confirming its strong oncogenic potential [82]. A c-Myc inhibitory peptide was first described by Draeger and Mullen [1], and it was chosen from a screen of rationally designed peptides based on the dimer interface between c-Myc and Max. c-Myc must bind with Max to make a functional transcription factor [83], and peptides from the dimer interface of each protein were tested for the ability to block DNA binding by c-Myc. The most potent inhibitor found in the screen was a mutated version of helix 1 (H1) from c-Myc, in which two native amino acids were mutated to alanine (H1 S6A, F8A). Giorello *et al.* attached the mutated H1 peptide to a cell penetrating peptide from Antp [67,84] in order to enhance its cellular uptake. They showed that the Antp-H1 peptide could block the c-Myc–Max interaction *in vitro*, and that the Antp-H1 peptide inhibited the proliferation of MCF-7 breast cancer cells grown in culture [2]. In an attempt to overcome the expected limitation of rapid degradation, they also synthesized a retro-inverso version of the Antp-H1 peptide using D amino acids and showed that it was 30 to 35 fold more stable and 5 to 10 fold more potent for inhibition of cell proliferation [85].

The ELP-based c-Myc inhibitory peptide was designed to include the penetratin cell penetrating peptide at the N-terminus of ELP and the c-Myc inhibitory peptide H1 (S6A, F8A) at the C-terminus (Pen-ELP-H1). Polypeptides were made to contain the thermally sensitive ELP1 as well as the control for polypeptide aggregation ELP2. In addition, control polypeptides lacking either the penetratin sequence or the H1 peptide were made. In order to determine the effects of the penetratin peptide and the ELP aggregation on cellular uptake, the level of polypeptide bound to and internalized by cells was evaluated using fluorescein labeled proteins and a flow cytometry assay. Pen-ELP1-H1, Pen-ELP2-H1, ELP1-H1 and ELP2-H1 were labeled with fluorescein on a single cysteine residue, and MCF-7 human breast carcinoma cells cultured *in vitro* were treated with the labeled proteins for 1 h at 37 or 42°C. At the end of the treatment, the level of fluorescein fluorescence was determined using flow cytometry. As shown in **Figure 4A**, the addition of the penetratin peptide to the construct resulted in at least a threefold increase in the amount of polypeptide associated with cells. Next, the effect of Pen–ELP1–H1 aggregation on its cellular association was determined. When treated at 42°C, the amount of Pen–ELP1–H1 bound to or inside the cells was 13-fold higher than in cells treated below the T_t at 37°C. Hyperthermia itself may affect cellular processes, including cellular uptake [86]. Therefore, to discriminate the effect of heat in stimulating the cellular uptake from that of the thermally triggered phase transition of Pen–ELP1–H1, a control experiment was performed in which the uptake of a fluorescein-labeled thermally non-responsive control polypeptide, Pen–ELP2–H1 was determined. As shown in **Figure 4A**, the uptake of Pen–ELP2–H1 in cells heated to 42°C was similar to uptake in non-heated cells, indicating that hyperthermia itself does not affect uptake of these polypeptides in cultured cells. In summary, these results demonstrate that the enhanced cellular uptake of thermally responsive Pen–ELP1–H1 in heated cells is not the result of non-specific effects of hyperthermia, but rather it is attributable to its hyperthermia triggered phase transition.

In order to further confirm the flow cytometry internalization results and to identify the intracellular localization of Pen–ELP–H1, the MCF-7 cells were examined by confocal fluorescence microscopy after polypeptide treatment. Cells were treated with rhodamine-labeled Pen–ELP1–H1 or Pen–ELP2–H1 for 1 h at 37 or 42°C and examined either immediately or 24 h later. Immediately after treatment, the Pen–ELP–H1 polypeptides were concentrated on the outer surface of the plasma membrane, and, in cells treated at 42°C, large aggregates of Pen–ELP1–H1 were visible outside the cell (**Figure 4B**). 24 h after treatment, Pen–ELP–H1 was internalized by the MCF-7 cells and was localized in a punctate staining pattern in the cell cytoplasm. In addition, large aggregates of Pen–ELP1–H1 could be seen in the cell cytoplasm after 42°C treatment (**Figure 4B**, lower right), confirming the internalization of even the large ELP aggregates. No such aggregates were seen in the absence of hyperthermia (**Figure 4B**, upper right) or after treatment with Pen–ELP2–H1 (data not shown), confirming that the aggregates formed were the result of the hyperthermia-induced ELP phase transition.

Once it was confirmed that Pen–ELP–H1 was internalized into cancer cells *in vitro*, its ability to inhibit the proliferation of these cells was assessed. In order to examine the effect of the penetratin peptide and the aggregation of ELP on cell proliferation, MCF-7 cells were treated with Pen–ELP1–H1, Pen–ELP2–H1 and the control polypeptides for 1 h at 37 and 42°C, then counted on day 11 using the trypan blue dye exclusion assay. **Figure 4C** shows that the control polypeptides lacking either the penetratin sequence or the H1 sequence had no effect on MCF-7 proliferation. When treated at 37°C, Pen–ELP1–H1 reduced proliferation by 35%. When treated at 42°C, the effect on proliferation was enhanced twofold to a 70% reduction in proliferation. Treatment with Pen–ELP2–H1 reduced proliferation by 25 – 30%, similar to Pen–ELP1–H1 at 37°C, and was not affected by hyperthermia treatment. These results demonstrate that Pen–ELP–H1 slows the growth of all cell lines tested, and that the effects of Pen–ELP1–H1 on cell proliferation can be enhanced by inducing aggregation of the polypeptide.

To investigate the mechanism of inhibition of cell proliferation by Pen–ELP1–H1, the cellular localization of

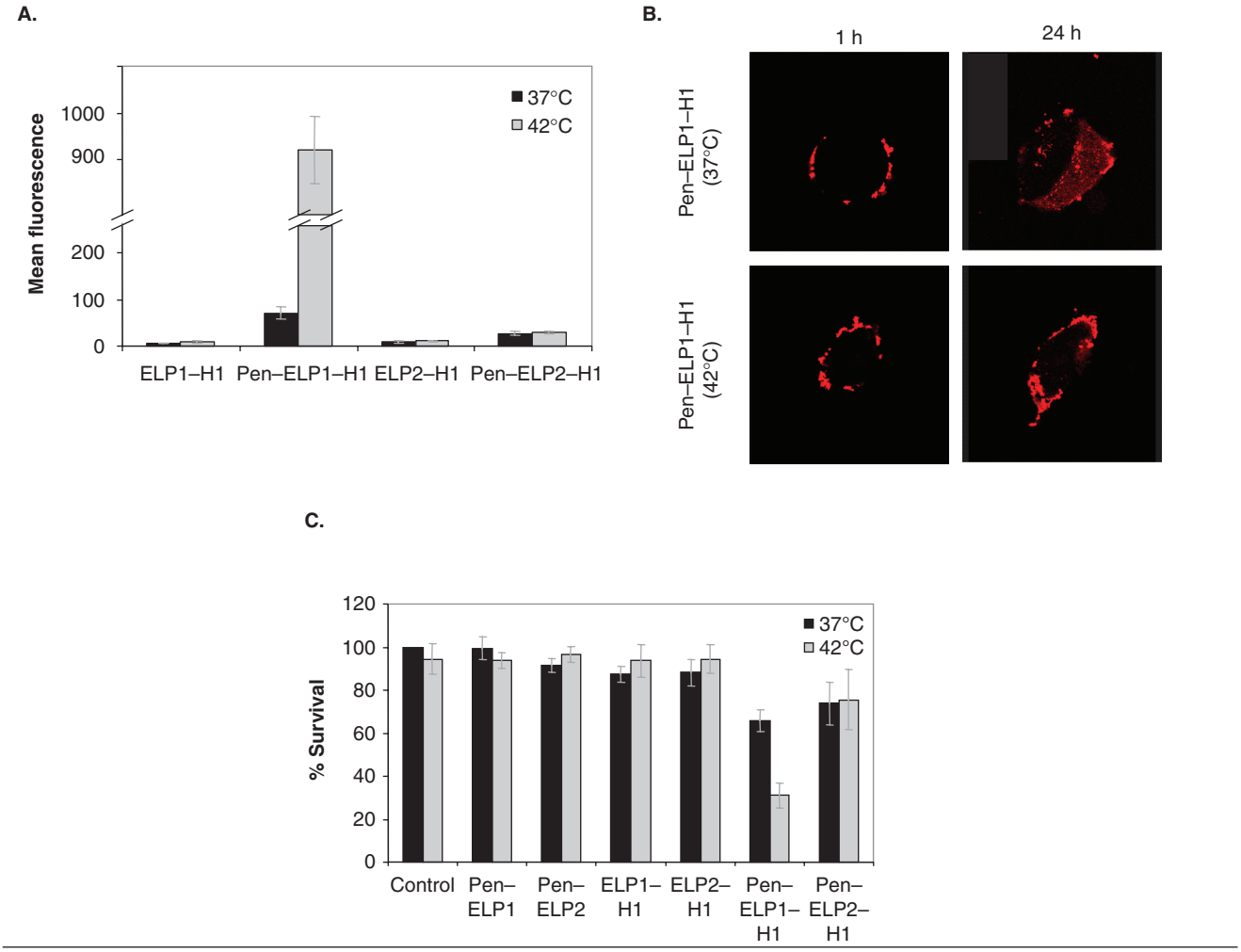

Figure 4. Delivery of a c-Myc inhibitory peptide using ELP (continued). A. Cellular uptake of Pen–ELP–H1. The effect of penetratin and hyperthermia on polypeptide uptake was determined by flow cytometry. Cells were treated for 1 h at 37°C or 42°C with fluorescein-labeled polypeptides (18 μM) and analyzed immediately after treatment. Results are expressed as fluorescence relative to standard beads, corrected for labeling efficiency, and represent the mean ± SE of three to five experiments (n = 5,000 cells). **B.** Localization and internalization of polypeptides. Cells were treated with 18 μM Pen–ELP1–H1 for 1 h at 37°C (top panel) or 42°C (bottom panel) and analyzed 1 h (left panel) or 24 h later (right panel) by confocal fluorescence microscopy. PMT voltages were adjusted during image acquisition to maximize image resolution. Therefore, the image intensity does not represent the quantitative amount of polypeptide in the cells. **C.** Antiproliferative effect of Pen–ELP–H1. Proliferation of MCF-7 cells was determined 11 days after a single 1 h treatment with the indicated polypeptide at 37 or 42°C. Cells were counted using the trypan blue dye exclusion assay. Results represent the mean ± SE of three to five experiments performed in duplicate.
ELP: Elastin-like polypeptide; SE: Standard error.

c-Myc and its dimerization partner Max was examined by confocal immunofluorescence microscopy in MCF-7 cells. **Figure 4D** (upper panel) shows that, in untreated cells, Max displays primarily a nuclear distribution exclusive of nucleoli (FITC channel, green). A similar distribution is as also observed for c-Myc (Cy5 channel, red), which is consistent with previous studies [87,88]. The overlay of images of Max and c-Myc (upper panel, third figure) shows nuclear colocalization of these two proteins, as indicated by the yellow color. The localization of c-Myc and Max is unchanged when cells are treated with Pen–ELP1 (middle panel). Treatment of cells with Pen–ELP1–H1 did not change the intracellular distribution of Max (lower panel, first figure). However, Pen–ELP1–H1 treatment caused redistribution of c-Myc from predominantly nuclear to cytoplasmic localization, thus preventing colocalization of Max and c-Myc (lower panel, second and third figures).

Since c-Myc–Max heterodimerization is required for c-Myc transcriptional activity, blocking the c-Myc–Max interaction may be an effective mode of inhibiting transcription of c-Myc responsive genes. The ability of Pen–ELP1–H1 to inhibit transcriptional activity of c-Myc was evaluated by assaying the mRNA expression of genes known to be direct targets of c-Myc. c-Myc responsive genes displaying

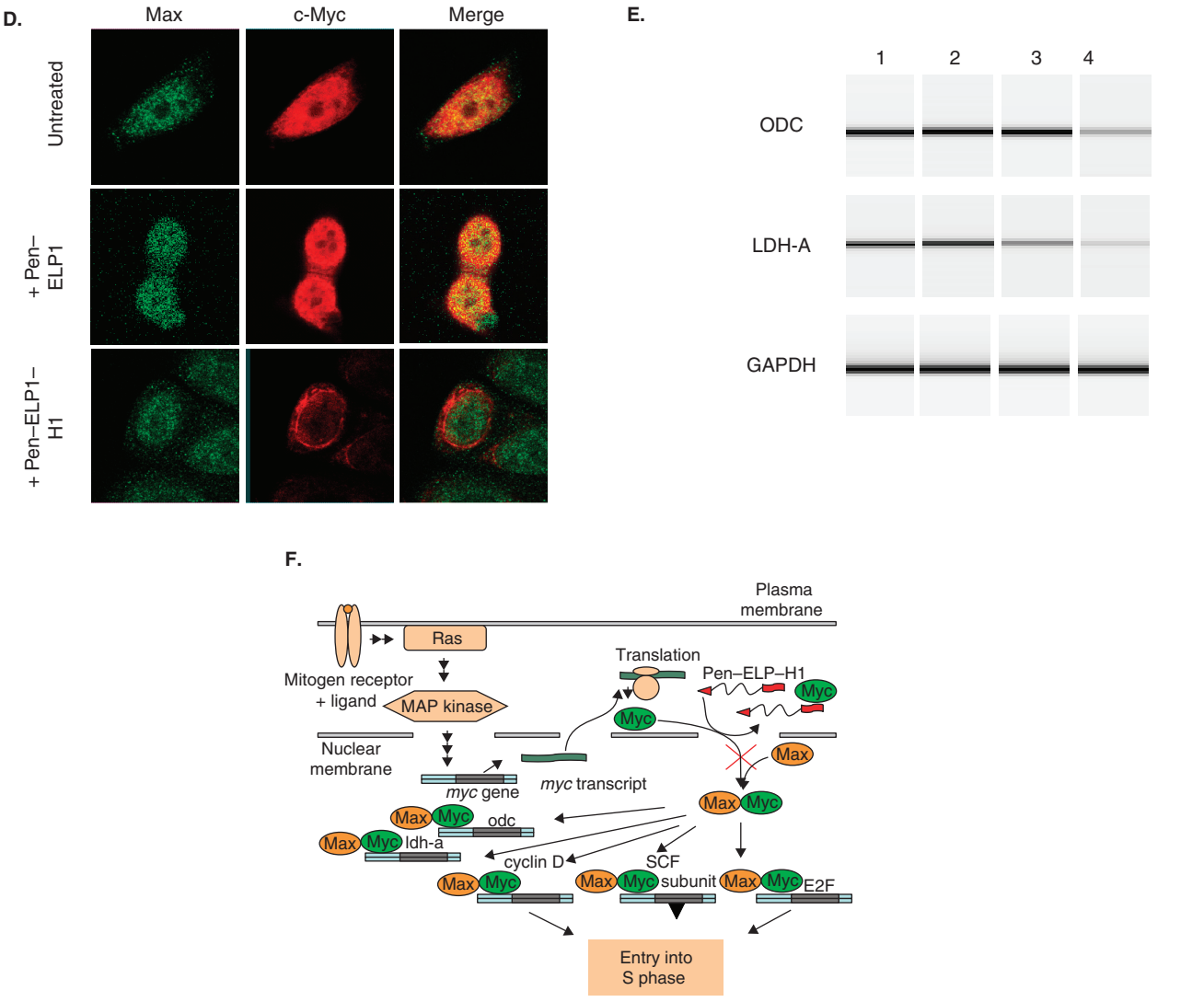

Figure 4. Delivery of a c-Myc inhibitory peptide using ELP (continued). D. Effect of Pen–ELP1–H1 on c-Myc localization. The subcellular localization of c-Myc and Max was determined by confocal immunofluorescence microscopy in untreated cells (top panel) and in cells treated with 18 μM Pen–ELP1 (middle panel) or 18 μM Pen–ELP1–H1 (bottom panel) for 1 h. Images were taken 24 h after polypeptide treatment with a 100× oil immersion objective. **E.** Effect of Pen–ELP1–H1 on c-Myc transcriptional activity. The mRNA levels for the c-Myc responsive genes ODC (top panel) and LDH-A (middle panel) and a control gene GAPDH (bottom panel) were assayed by RT–PCR. MCF-7 cells were untreated (lane 1) or treated with 18 μM Pen–ELP1 (lane 2), ELP1–H1 (lane 3), or Pen–ELP1–H1 (lane 4) for 1 h. RNA was purified 48 h after treatment. PCR products were analyzed by capillary electrophoresis using a Bioanalyzer Labchip with fluorescence detection. The fluorescence data was converted to a simulated gel using Agilent software. **F.** Proposed model for c-Myc inhibition by Pen–ELP–H1. Mitogen stimulation induces transcription of mRNA from the c-Myc gene. After translation of the c-Myc protein in the cytoplasm, it is bound by the Pen–ELP–H1 polypeptide. Once bound, c-Myc can not be imported into the nucleus and interact with Max. This results in the downregulation of c-Myc–Max responsive genes and leads to inhibition of cell proliferation.

ELP: Elastin-like polypeptide; SE: Standard error.

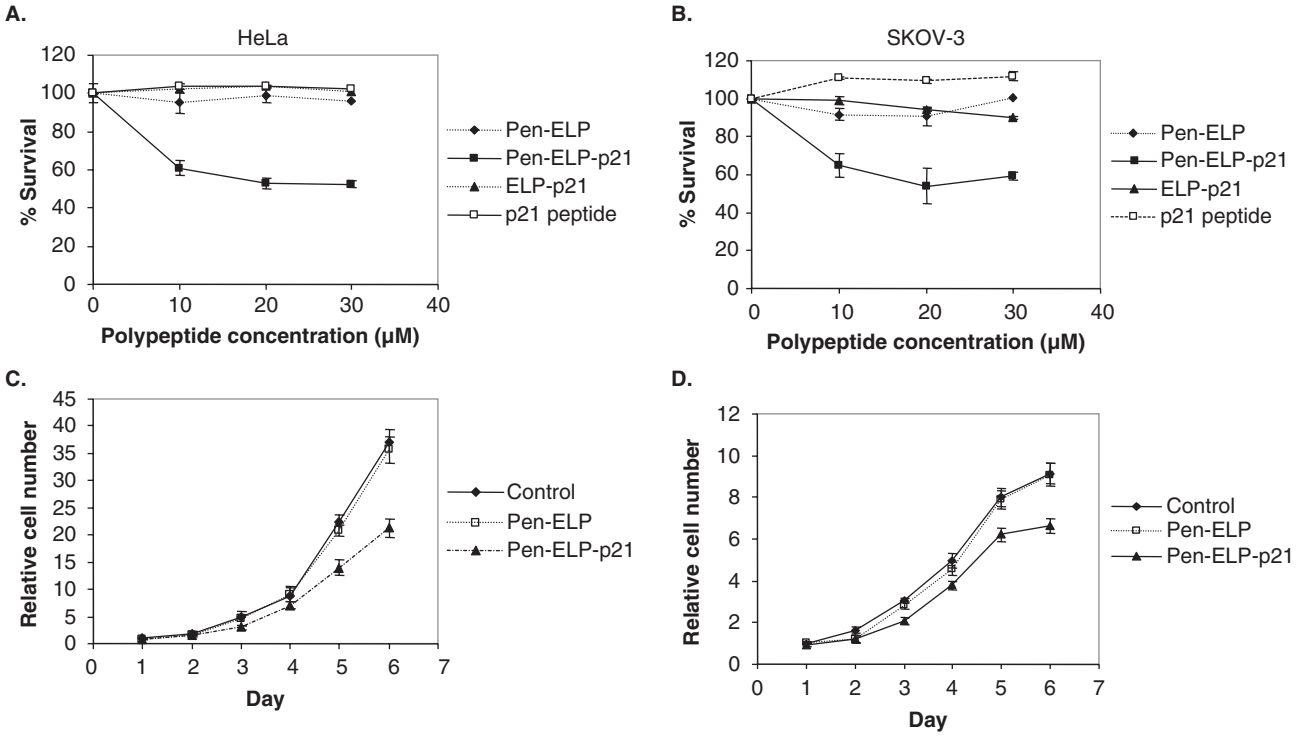

Figure 5. Effect of Pen–ELP–p21 on cell proliferation. A. and **B.** Cell proliferation in HeLa and SKOV-3 cells, respectively, as measured by the MTS assay 72 h after polypeptide treatment. **C.** and **D.** Proliferation curves of HeLa and SKOV-3 cells, respectively, after treatment with 20 μM Pen–ELP–p21 for 72 h. Cell numbers are expressed relative to the count on day 1. Results are represented as mean ± SEM of three independent experiments.
ELP: Elastin-like polypeptide; SEM: Standard error of the mean.

c-Myc–Max binding sites in their promoters include ornithine decarboxylase (ODC) [89] and lactate dehydrogenase-A (LDH-A) [90]. Expression levels of ODC and LDH-A mRNA from treated and untreated cells were analyzed by RT–PCR and compared with the expression of glyceraldehyde phosphate dehydrogenase (GAPDH), a gene not regulated by c-Myc. The control polypeptide Pen–ELP1 did not show any inhibition of c-Myc transcriptional activity (**Figure 4E**, lane 2). The control polypeptide ELP1–H1 also showed no significant effect (lane 3). In contrast, Pen–ELP1–H1 led to a strong decrease in mRNA expression of ODC and LDH-A (lane 4). GAPDH mRNA levels were unaffected by the polypeptide treatments.

The redistribution of c-Myc to the cytoplasm and the downregulation of c-Myc controlled genes led to the proposed model illustrated in **Figure 4F**. Mitogen-induced cell proliferation stimulates production of c-Myc mRNA. c-Myc protein is translated in the cytoplasm, but before it is imported into the nucleus, it is sequestered by the cytoplasmically localized Pen–ELP–H1. The nascent c-Myc cannot enter the nucleus, therefore leaving Max without a binding partner. The result is the downregulation of c-Myc–Max controlled genes. The c-Myc protein has a high turnover rate [83], which explains why c-Myc staining is exclusively in the cytoplasm only 24 h after treatment. Without a functional c-Myc–Max heterodimer, the processes of cell growth and cell proliferation are inhibited.

2.6 Delivery of a p21 mimetic peptide by ELP

p21 is a cyclin-dependent kinase inhibitor which plays an important role in regulation of the cell cycle. In response to DNA damage, p21 expression can induce cell cycle arrest, which leads to an apoptotic response. A p21 mimetic peptide was first described by Ball *et al.* [91]. The authors carried out a systematic study to examine a library of synthetic peptides based on the sequence of $p21^{WAF1}$. They checked the ability of various peptides to interact with and inhibit the cyclin D1–CDK4 interaction. The authors reported that peptides corresponding to the carboxy terminus of p21 showed an inhibitory effect when introduced into human-keratinocyte-derived HaCaT cells [91]. In a separate study, Mutoh *et al.* [50] showed that a smaller section of the peptide used by Ball *et al.*, comprising amino acids 139 – 164, was a potent inhibitor of cyclin D1-CDK4 and cyclin E-CDK2 kinase activity. They also demonstrated a decrease in cell growth of CA46 human lymphoma cells when treated with the p21 peptide fused to the cell penetrating peptide Pen [50]. The C-terminal portion of

p21 has also been shown to bind to proliferating cell nuclear antigen (PCNA). Mattock *et al.* expressed a GFP–p21 miniprotein fusion complex which bound to PCNA and inhibited colony formation of different mammalian cell lines [92]. Another study showing the potential of the Tat cell penetrating peptide to deliver cargo inside the cell, attached the PCNA binding domain of $p21^{WAF/CIP}$ to Tat. This Tat–p21 fusion complex was able to decelerate mouse myoblasts cell cycle progression. The authors theorized that inhibition was due to the p21–PCNA interaction [93]. In a similar study, Baker *et al.* conjugated Tat with p21 and showed that it caused a decrease in cell proliferation of U251 (glioblastoma), U373 (astrocytoma), MCF-7 (breast carcinoma) and SW480 (colorectal adenocarcinoma) cell lines. They also showed the colocalization of Tat-p21 with PCNA in the nucleus of the U251 human glioblastoma cells. They further proposed that Tat–p21 disrupted PCNA function and thereby caused cell toxicity by apoptosis [94].

In order to enhance the cellular delivery of the p21 mimetic peptide first described by Mutoh *et al.* [50], Massodi *et al.* expressed it as a fusion polypeptide at the C-terminus of Pen–ELP [57]. In order to show that the Pen–ELP–p21 polypeptide treatment was able to inhibit proliferation of different cell lines, HeLa and SKOV-3 cells were treated with Pen–ELP–p21 and other control polypeptides lacking p21 in a concentration dependent manner. The cell proliferation was measured by MTS assay 72 h later. It was observed that there was a decrease in the number of viable cells after treatment with Pen–ELP–p21 in a concentration-dependent manner in both HeLa and SKOV-3 cells. On the other hand, cells treated with control polypeptides were not affected (**Figure 5A** and **B**). This inhibition of HeLa and SKOV-3 cell proliferation was further confirmed by measuring the proliferation rate of cells in the presence of 20 μM Pen–ELP–p21 and other control polypeptides. As shown in **Figure 5C**, HeLa cells treated with Pen–ELP–p21 showed a decreased proliferation rate as compared to untreated and Pen–ELP-treated cells. This result was confirmed in SKOV-3 cells (**Figure 5D**). These results suggest that Pen–ELP is an effective vehicle for p21 peptide delivery.

3. Conclusion

The work described here establishes the groundwork for the use of ELP for thermally targeted delivery of both small molecule drugs and inhibitory peptides. Evaluation of both strategies *in vivo* is ongoing and, if successful, the ELP approach could allow tumor-specific delivery of potentially any therapeutic molecule. This work has great implications for the future of ELP-mediated drug delivery. This technique will improve the efficacy of cancer therapy and reduce the side effects, which will lead to a better quality of life for chemotherapy patients.

4. Expert opinion

Elastin-like polypeptide is emerging as an effective means to deliver a diverse array of therapeutic molecules in a hyperthermia targeted manner. The work highlighted in this review shows that ELP has the potential to deliver both small molecule chemotherapeutics and bioactive peptides. ELP is an optimized macromolecular carrier because it exhibits all the positive attributes of a high molecular weight drug carrier, including extended plasma half life, enhanced drug solubility, passive tumor targeting, reduced systemic drug toxicity and evasion of multidrug resistance. And, it further improves on classical synthetic macromolecules in that the sequence and molecular weight can be precisely controlled, it can be expressed in *E. coli* and, most importantly, it is thermally responsive. The ELP-fused therapeutic peptides are especially promising because they combine the physical targeting of ELP to the tumor site with the molecular targeting of the therapeutic peptide to its intracellular target, often a protein aberrantly functioning in the cancer cell. The long plasma half-life and ability of ELP to be concentrated in tumor tissue by focused hyperthermia *in vivo* have been demonstrated in several studies published by Dr Chilkoti's group. Further development of the ELP drug carrier depends on addressing several key issues in an animal model. The ability of ELP fused to a therapeutic molecule to reduce tumor size has not been published to date. A common setback for protein-based therapies is induction of an immune response from the host. The toxicity and immunogenicity of the polypeptide needs to be examined. Also, although it has been determined that ELP escapes the tumor vasculature, its ability to traverse the tumor cells' plasma membrane needs to be demonstrated. The use of ELPs fused to cell penetrating peptides should prove very useful for crossing this hurdle. Studies are currently underway in our laboratory to address these issues. Preliminary studies with Tat–ELP–GFLG–Dox have shown that this polypeptide is capable of reducing the size of MES-SA tumors grown in nude rats, and the ELP-fused Dox is less toxic, as judged by body weight loss and injection site necrosis, than free Dox (unpublished data). Additional preliminary studies utilizing subcutaneous xenografts in rats and fluorescently labeled Tat–ELP have shown that the polypeptide is not only capable of escaping the tumor vasculature, but it can also enter the cytoplasm of the tumor cells (unpublished data). Completion of these studies, as well as further examination of the ability of ELP-delivered therapeutics to reduce tumor size, will provide the necessary data to advance the ELP technology toward the ultimate goal of human therapeutics.

Declaration of interest

This work was partially supported by a research grant from the Milheim Foundation for Cancer Research to Gene Bidwell. In addition, the work was partially supported using grant R21 CA113813-01A2 from the National Institutes of Health, a Wendy Will Case Cancer Foundation grant, and an American Cancer Society Institutional Research Grant to the University of Mississippi Medical Center and Drazen Raucher. Raucher also is affiliated as a sub-award contractor with Houston Pharmaceuticals, Inc. (Houston, TX) for grant R43 CA126318-01A1, and Raucher is affiliated with Thermally Targeted Therapeutics, which is developing ELP-based technology for targeted drug delivery.

Bibliography

Papers of special note have been highlighted as either of interest (•) or of considerable interest (••) to readers.

1. Draeger LJ, Mullen GP. Interaction of the bHLH-zip domain of c-Myc with H1-type peptides. Characterization of helicity in the H1 peptides by NMR. J Biol Chem 1994;269(3):1785-93
2. Giorello L, Clerico L, Pescarolo MP, et al. Inhibition of cancer cell growth and c-Myc transcriptional activity by a c-Myc helix 1-type peptide fused to an internalization sequence. Cancer Res 1998;58(16):3654-9
• **This article describes the ability of a peptide derived from c-Myc to inhibit transcriptional activity and cell proliferation.**
3. Clark GJ, Drugan JK, Terrell RS, et al. Peptides containing a consensus Ras binding sequence from Raf-1 and the GTPase activating protein NF1 inhibit Ras function. Proc Natl Acad Sci USA 1996;93(4):1577-81
4. Rojas M, Yao S, Lin YZ. Controlling epidermal growth factor (EGF)-stimulated Ras activation in intact cells by a cell-permeable peptide mimicking phosphorylated EGF receptor. J Biol Chem 1996;271(44):27456-61
5. Khalil MW, Sasse F, Lunsdorf H, et al. Mechanism of action of tubulysin, an antimitotic peptide from myxobacteria. Chembiochem 2006;7(4):678-83
6. Ellerby HM, Arap W, Ellerby LM, et al. Anti-cancer activity of targeted pro-apoptotic peptides. Nat Med 1999;5(9):1032-8
7. Friedman PN, McAndrew SJ, Gawlak SL, et al. BR96 sFv-PE40, a potent single-chain immunotoxin that selectively kills carcinoma cells. Cancer Res 1993;53(2):334-9
8. Kashiwagi H, McDunn JE, Goedegebuure PS, et al. TAT-Bim induces extensive apoptosis in cancer cells. Ann Surg Oncol 2007
9. Oh KJ, Barbuto S, Pitter K, et al. A membrane-targeted BID BCL-2 homology 3 peptide is sufficient for high potency activation of BAX in vitro. J Biol Chem 2006;281(48):36999-7008
10. Prive GG, Melnick A. Specific peptides for the therapeutic targeting of oncogenes. Curr Opin Genet Dev 2006;16(1):71-7
11. Talmadge JE. Pharmacodynamic aspects of peptide administration biological response modifiers. Adv Drug Deliv Rev 1998;33(3):241-52
12. Lipka E, Crison J, Amidon GL. Transmembrane transport of peptide type compounds: prospects for oral delivery. J Control Rel 1996;39(2-3):121-9
13. Chandran SS, Nan A, Rosen DM, et al. A prostate-specific antigen activated N-(2-hydroxypropyl) methacrylamide copolymer prodrug as dual-targeted therapy for prostate cancer. Mol Cancer Ther 2007;6(11):2928-37
14. Urry DW, Luan C-H, Parker TM, et al. Temperature of polypeptide inverse temperature transition depends on mean residue hydrophobicity. J Am Chem Soc 1991;113:4346-8
15. Meyer DE, Kong GA, Dewhirst MW, et al. Targeting a genetically engineered elastin-like polypeptide to solid tumors by local hyperthermia. Cancer Res 2001;61(4):1548-54
• **This article was the first *in vivo* demonstration that ELP can be targeted to the tumor site using hyperthermia.**
16. Allen TM. Liposomal drug formulation: rationale for development and what we can expect in the future. Drugs 1998;56:747-56
17. Kissel M, Peschke P, Subr V, et al. Synthetic macromolecular drug carriers: biodistribution of poly[(N-2-hydroxypropyl)methacrylamide] copolymers and their accumulation in solid rat tumors. PDA J Pharm Sci Technol 2001;55(3):191-201
18. Bidwell GL 3rd, Raucher D. Application of thermally responsive polypeptides directed against c-Myc transcriptional function for cancer therapy. Mol Cancer Ther 2005;4(7):1076-85
•• **This article describes the ability of ELP to deliver the c-Myc inhibitory peptide.**
19. Chow DC, Dreher MR, Trabbic-Carlson K, et al. Ultra-high expression of a thermally responsive recombinant fusion protein in E. coli. Biotechnol Prog 2006;22(3):638-46
20. Cassidy J, Duncan R, Morrison GJ, et al. Activity of N-(2-hydroxypropyl) methacrylamide copolymers containing daunomycin against a rat tumour model. Biochem Pharmacol 1989;38(6):875-9
21. Maeda H, Seymour LW, Miyamoto Y. Conjugates of anticancer agents and polymers: advantages of macromolecular therapeutics in vivo. Bioconjug Chem 1992;3(5):351-62
22. Takakura Y, Fujita T, Hashida M, et al. Disposition characteristics of macromolecules in tumor-bearing mice. Pharm Res 1990;7(4):339-46
23. Yamaoka T, Tabata Y, Ikada Y. Distribution and tissue uptake of poly(ethylene glycol) with different molecular weights after intravenous administration to mice. J Pharm Sci 1994;83(4):601-6
24. Yowell SL, Blackwell S. Novel effects with polyethylene glycol modified pharmaceuticals. Cancer Treat Rev 2002;28(Suppl A):3-6
25. Burnham NL. Polymers for delivering peptides and proteins. Am J Hosp Pharm 1994;51(2):210-8; quiz 28-9
26. Duncan R, Coatsworth JK, Burtles S. Preclinical toxicology of a novel polymeric antitumour agent: HPMA copolymer-doxorubicin (PK1). Hum Exp Toxicol 1998;17(2):93-104
27. Seymour LW, Duncan R, Kopeckova P, et al. Daunomycin- and adriamycin-N-(2-hydroxypropyl)methacrylamide copolymer

conjugates; toxicity reduction by improved drug-delivery. Cancer Treat Rev 1987;14(3-4):319-27

28. Yeung TK, Hopewell JW, Simmonds RH, et al. Reduced cardiotoxicity of doxorubicin given in the form of N-(2-hydroxypropyl) methacrylamide conjugates: and experimental study in the rat. Cancer Chemother Pharmacol 1991;29(2):105-11
29. St'astny M, Strohalm J, Plocova D, et al. A possibility to overcome P-glycoprotein (PGP)-mediated multidrug resistance by antibody-targeted drugs conjugated to N-(2-hydroxypropyl)methacrylamide (HPMA) copolymer carrier. Eur J Cancer 1999;35(3):459-66
30. Ryser HJ, Shen WC. Conjugation of methotrexate to poly(L-lysine) increases drug transport and overcomes drug resistance in cultured cells. Proc Natl Acad Sci USA 1978;75(8):3867-70
31. Ohkawa K, Hatano T, Yamada K, et al. Bovine serum albumin-doxorubicin conjugate overcomes multidrug resistance in a rat hepatoma. Cancer Res 1993;53(18):4238-42
32. Minko T, Kopeckova P, Pozharov V, et al. HPMA copolymer bound adriamycin overcomes MDR1 gene encoded resistance in a human ovarian carcinoma cell line. J Control Rel 1998;54(2):223-33
33. Urry DW. Free energy transduction in polypeptides and proteins based on inverse temperature transitions. Prog Biophys Mol Biol 1992;57(1):23-57
34. Liu W, Dreher MR, Furgeson DY, et al. Tumor accumulation, degradation and pharmacokinetics of elastin-like polypeptides in nude mice. J Control Rel 2006

• **This article offers further demonstration of ELP pharmacokinetics and thermal targeting *in vivo*.**

35. Dreher MR, Liu W, Michelich CR, et al. Thermal cycling enhances the accumulation of a temperature-sensitive biopolymer in solid tumors. Cancer Res 2007;67(9):4418-24
36. Marco A, Arcamone F. DNA complexing antibiotics: daunomycin, adriamycin and their derivatives. Arzneimittelforschung 1975;25(3):368-74
37. Ross WE, Bradley MO. DNA double-stranded breaks in mammalian cells after exposure to intercalating agents. Biochim Biophys Acta 1981;654(1):129-34
38. Ling YH, Priebe W, Perez-Soler R. Apoptosis induced by anthracycline antibiotics in P388 parent and multidrug-resistant cells. Cancer Res 1993;53(8):1845-52
39. Handa K, Sato S. Generation of free radicals of quinone group-containing anti-cancer chemicals in NADPH-microsome system as evidenced by initiation of sulfite oxidation. Gann 1975;66(1):43-7
40. Goodman J, Hochstein P. Generation of free radicals and lipid peroxidation by redox cycling of adriamycin and daunomycin. Biochem Biophys Res Commun 1977;77(2):797-803
41. Myers CE, McGuire WP, Liss RH, et al. Adriamycin: the role of lipid peroxidation in cardiac toxicity and tumor response. Science 1977;197(4299):165-7
42. Triton TR, Yee G. The anticancer agent adriamycin can be actively cytotoxic without entering cells. Science 1982;217(4556):248-50
43. Olson HM, Capen CC. Chronic cardiotoxicity of doxorubicin (adriamycin) in the rat: morphologic and biochemical investigations. Toxicol Appl Pharmacol 1978;44(3):605-16
44. Olson HM, Capen CC. Subacute cardiotoxicity of adriamycin in the rat: biochemical and ultrastructural investigations. Lab Invest 1977;37(4):386-94
45. Olson RD, Boerth RC, Gerber JG, et al. Mechanism of adriamycin cardiotoxicity: evidence for oxidative stress. Life Sci 1981;29(14):1393-401
46. Olson RD, Mushlin PS. Doxorubicin cardiotoxicity: analysis of prevailing hypotheses. FASEB J 1990;4(13):3076-86
47. Denny WA. DNA-intercalating ligands as anti-cancer drugs: prospects for future design. Anticancer Drug Des 1989;4(4):241-63
48. Dano K. Active outward transport of daunomycin in resistant Ehrlich ascites tumor cells. Biochim Biophys Acta 1973;323(3):466-83
49. Long SB, Hancock PJ, Kral AM, et al. The crystal structure of human protein farnesyltransferase reveals the basis for inhibition by CaaX tetrapeptides and their mimetics. Proc Natl Acad Sci USA 2001;98(23):12948-53
50. Mutoh M, Lung FD, Long YQ, et al. A p21(Waf1/Cip1)carboxyl-terminal peptide exhibited cyclin-dependent kinase-inhibitory activity and cytotoxicity when introduced into human cells. Cancer Res 1999;59(14):3480-8
51. Bonfanti M, Taverna S, Salmona M, et al. p21WAF1-derived peptides linked to an internalization peptide inhibit human cancer cell growth. Cancer Res 1997;57(8):1442-6
52. Selivanova G, Iotsova V, Okan I, et al. Restoration of the growth suppression function of mutant p53 by a synthetic peptide derived from the p53 C-terminal domain. Nat Med 1997;3(6):632-8
53. Wang B, Yang H, Liu YC, et al. Isolation of high-affinity peptide antagonists of 14-3-3 proteins by phage display. Biochemistry 1999;38(38):12499-504
54. Blondelle SE, Houghten RA. Design of model amphipathic peptides having potent antimicrobial activities. Biochemistry 1992;31(50):12688-94
55. Leuschner C, Hansel W. Membrane disrupting lytic peptides for cancer treatments. Curr Pharm Des 2004;10(19):2299-310
56. Lee DG, Kim HN, Park Y, et al. Design of novel analogue peptides with potent antibiotic activity based on the antimicrobial peptide, HP (2-20), derived from N-terminus of Helicobacter pylori ribosomal protein L1. Biochim Biophys Acta 2002;1598(1-2):185-94
57. Massodi I, Bidwell GL 3rd, Raucher D. Evaluation of cell penetrating peptides fused to elastin-like polypeptide for drug delivery. J Control Rel 2005;108(2-3):396-408

• **This article describes the use of cell penetrating peptides to enhance the cellular uptake of ELP.**

58. Liu W, Dreher MR, Chow DC, et al. Tracking the in vivo fate of recombinant polypeptides by isotopic labeling. J Control Rel 2006;114(2):184-92
59. Fujiwara K, Watanabe T. Effects of hyperthermia, radiotherapy and thermoradiotherapy on tumor microvascular permeability. Acta Pathol Jpn 1990;40(2):79-84
60. Gerlowski LE, Jain RK. Effect of hyperthermia on microvascular

permeability to macromolecules in normal and tumor tissues. Int J Microcirc Clin Exp 1985;4(4):363-72

61. Jain RK. Transport of molecules across tumor vasculature. Cancer Metastasis Rev 1987;6(4):559-93
62. Raucher D, Chilkoti A. Enhanced uptake of a thermally responsive polypeptide by tumor cells in response to its hyperthermia mediated phase transition. Cancer Res 2001;In press
63. Meyer DE, Shin BC, Kong GA, et al. Drug targeting using thermally responsive polymers and local hyperthermia. J Control Rel 2001;74(1-3):213-24
64. Graslund A, Eriksson LE. Properties and applications of cell-penetrating peptides. Genet Eng (NY) 2004;26:19-31
65. Derossi D, Joliot AH, Chassaing G, et al. The third helix of the Antennapedia homeodomain translocates through biological membranes. J Biol Chem 1994;269(14):10444-50
66. Weeks BS, Desai K, Loewenstein PM, et al. Identification of a novel cell attachment domain in the HIV-1 Tat protein and its 90-kDa cell surface binding protein. J Biol Chem 1993;268(7):5279-84
67. Hawiger J. Noninvasive intracellular delivery of functional peptides and proteins. Curr Opin Chem Biol 1999;3(1):89-94
68. Saalik P, Elmquist A, Hansen M, et al. Protein cargo delivery properties of cell-penetrating peptides. A comparative study. Bioconjug Chem 2004;15(6):1246-53
69. Silhol M, Tyagi M, Giacca M, et al. Different mechanisms for cellular internalization of the HIV-1 Tat-derived cell penetrating peptide and recombinant proteins fused to Tat. Eur J Biochem 2002;269(2):494-501
70. van Deurs B, Petersen OW, Olsnes S, et al. The ways of endocytosis. Int Rev Cytol 1989;117:131-77
71. Sandvig K, van Deurs B. Endocytosis without clathrin. Trends Cell Biol 1994;4(8):275-7
72. Sandvig K, van Deurs B. Endocytosis without clathrin (a minireview). Cell Biol Int Rep 1991;15(1):3-8
73. Heuser JE, Anderson RG. Hypertonic media inhibit receptor-mediated endocytosis by blocking clathrin-coated pit formation. J Cell Biol 1989;108(2):389-400
74. Thyberg J. Caveolae and cholesterol distribution in vascular smooth muscle cells of different phenotypes. J Histochem Cytochem 2002;50(2):185-95
75. Dreher MR, Raucher D, Balu N, et al. Evaluation of an elastin-like polypeptide-doxorubicin conjugate for cancer therapy. J Control Rel 2003;91(1-2):31-43

• **This article was the first to describe ELP delivery of doxorubicin.**

76. Minko T, Kopeckova P, Kopecek J. Efficacy of the chemotherapeutic action of HPMA copolymer-bound doxorubicin in a solid tumor model of ovarian carcinoma. Int J Cancer 2000;86(1):108-17
77. Kopecek J, Kopeckova P, Minko T, et al. HPMA copolymer-anticancer drug conjugates: design, activity, and mechanism of action. Eur J Pharm Biopharm 2000;50(1):61-81
78. Furgeson DY, Dreher MR, Chilkoti A. Structural optimization of a "smart" doxorubicin-polypeptide conjugate for thermally targeted delivery to solid tumors. J Control Rel 2006;110(2):362-9
79. Bidwell GL 3rd, Fokt I, Priebe W, et al. Development of elastin-like polypeptide for thermally targeted delivery of doxorubicin. Biochem Pharmacol 2007;73(5):620-31

•• **This article describes the ability of ELP to deliver doxorubicin in a thermally targeted manner.**

80. Duncan R, Cable HC, Lloyd JB, et al. Degradation of side-chains of N-(2-hydroxypropyl)methacrylamide copolymers by lysosomal thiol-proteinases. Biosci Rep 1982;2(12):1041-6
81. Bidwell GL, Davis AN, Fokt I, et al. A thermally targeted elastin-like polypeptide – doxorubicin conjugate overcomes drug resistance. Inv New Drugs 2007;In press

•• **This article describes the ability of ELP-delivered doxorubicin to accumulate in and kill doxorubicin resistant cells.**

82. Pelengaris S, Khan M, Evan G. c-MYC: more than just a matter of life and death. Nat Rev Cancer 2002;2(10):764-76
83. Blackwood EM, Luscher B, Eisenman RN. Myc and Max associate in vivo. Genes Dev 1992;6(1):71-80
84. Schwartz JJ, Zhang S. Peptide-mediated cellular delivery. Curr Opin Mol Ther 2000;2(2):162-7
85. Pescarolo MP, Bagnasco L, Malacarne D, et al. A retro-inverso peptide homologous to helix 1 of c-Myc is a potent and specific inhibitor of proliferation in different cellular systems. FASEB J 2001;15(1):31-3
86. Hildebrandt B, Wust P, Ahlers O, et al. The cellular and molecular basis of hyperthermia. Crit Rev Oncol Hematol 2002;43(1):33-56
87. Soldani C, Bottone MG, Biggiogera M, et al. Nuclear localization of phosphorylated c-Myc protein in human tumor cells. Eur J Histochem 2002;46(4):377-80
88. Abrams HD, Rohrschneider LR, Eisenman RN. Nuclear location of the putative transforming protein of avian myelocytomatosis virus. Cell 1982;29(2):427-39
89. Walhout AJ, Gubbels JM, Bernards R, et al. c-Myc/Max heterodimers bind cooperatively to the E-box sequences located in the first intron of the rat ornithine decarboxylase (ODC) gene. Nucleic Acids Res 1997;25(8):1516-25
90. Shim H, Dolde C, Lewis BC, et al. c-Myc transactivation of LDH-A: implications for tumor metabolism and growth. Proc Natl Acad Sci USA 1997;94(13):6658-63
91. Ball KL, Lain S, Fahraeus R, et al. Cell-cycle arrest and inhibition of Cdk4 activity by small peptides based on the carboxy-terminal domain of p21WAF1. Curr Biol 1997;7(1):71-80
92. Mattock H, Lane DP, Warbrick E. Inhibition of cell proliferation by the PCNA-binding region of p21 expressed as a GFP miniprotein. Exp Cell Res 2001;265(2):234-41
93. Tunnemann G, Martin RM, Haupt S, et al. Cargo-dependent mode of uptake and bioavailability of TAT-containing proteins and peptides in living cells. FASEB J 2006;20(11):1775-84
94. Baker RD, Howl J, Nicholl ID. A sychnological cell penetrating peptide mimic of p21(WAF1/CIP1) is pro-apoptogenic. Peptides 2007;28(4):731-40

Affiliation

Drazen Raucher[†,1], Iqbal Massodi[2] &
Gene L Bidwell III[3]
[†]Author for correspondence
[1]Associate Professor,
University of Mississippi Medical Center,
Department of Biochemistry,
2500 North State Street,
Jackson, MS 39216, USA
Tel: +1 601 984 1510; Fax: +1 601 984 1501;
E-mail: draucher@biochem.umsmed.edu
[2]Graduate Student,
University of Mississippi Medical Center,
Department of Biochemistry,
2500 North State Street,
Jackson, MS 39216, USA
E-mail: imassodi@biochem.umsmed.edu
[3]Postdoctoral Fellow,
University of Mississippi Medical Center,
Department of Biochemistry,
2500 North State Street,
Jackson, MS 39216, USA
E-mail: gbidwell@biochem.umsmed.edu